Volume 14 | Number 25 | 7 July 2018 | Pages 5153–5334

Soft Matter

rsc.li/soft-matter-journal

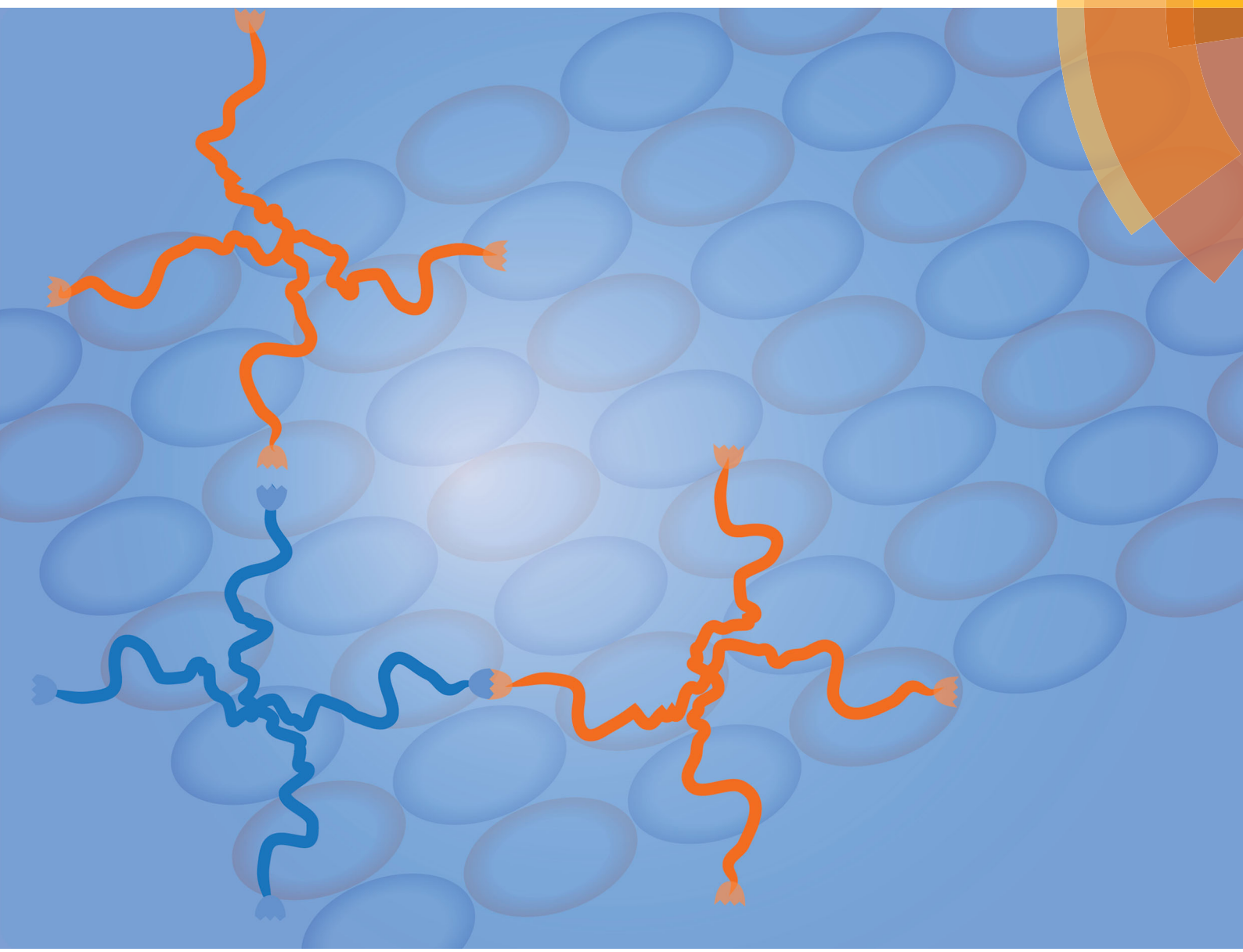

ISSN 1744-6848

ROYAL SOCIETY OF CHEMISTRY

PAPER
German Alberto Parada and Xuanhe Zhao
Ideal reversible polymer networks

Soft Matter

PAPER

View Article Online
View Journal | View Issue

Cite this: *Soft Matter*, 2018, **14**, 5186

Ideal reversible polymer networks

German Alberto Parada [ab] and Xuanhe Zhao *[bc]

In this article we introduce the concept of ideal reversible polymer networks, which have well-controlled polymer network structures similar to ideal covalent polymer networks but exhibit viscoelastic behaviors due to the presence of reversible crosslinks. We first present a theory to describe the mechanical properties of ideal reversible polymer networks. Because short polymer chains of equal length are used to construct the network, there are no chain entanglements and the chains' Rouse relaxation time is much shorter than the reversible crosslinks' characteristic time. Therefore, the ideal reversible polymer network behaves as a single Maxwell element of a spring and a dashpot in series, with the instantaneous shear modulus and relaxation time determined by the concentration of elastically-active chains and the dynamics of reversible crosslinks, respectively. The theory provides general methods to (i) independently control the instantaneous shear modulus and relaxation time of the networks, and to (ii) quantitatively measure kinetic parameters of the reversible crosslinks, including reaction rates and activation energies, from macroscopic viscoelastic measurements. To validate the proposed theory and methods, we synthesized and characterized the mechanical properties of a hydrogel composed of 4-arm polyethylene glycol (PEG) polymers end-functionalized with reversible crosslinks. All the experiments conducted by varying pH, temperature and polymer concentration were consistent with the predictions of our proposed theory and methods for ideal reversible polymer networks.

Received 27th March 2018,
Accepted 10th May 2018

DOI: 10.1039/c8sm00646f

rsc.li/soft-matter-journal

Introduction

While most crosslinked polymer networks are heterogeneous and lack controlled structure, ideal covalent polymer networks have been recently reported. The ideal covalent networks feature well-defined lengths of polymer chains, crosslink functionalities and network architectures.[7,8] To fabricate such networks, multi-arm (3 or 4-arm, typically) end-functionalized macromers of low molecular weight are mixed near the overlap concentration and crosslinked *via* a reaction of the end groups (Fig. 1a). These ideal covalent polymer networks not only provide powerful tools to study structure–property relationships of crosslinked polymers but also give elastomers and gels with well-controlled mechanical properties such as elasticity,[9–11] mesh size, stretchability[1,2,10,12,13] and fracture toughness.[14] But due to the permanent nature of the crosslinks, these network do not exhibit any viscoelasticity. To obtain viscoelastic properties, reversible crosslinks can be introduced.

Reversible crosslinking motifs, which include dynamic covalent bonds, metal–ligand coordination, hydrogen bonding domains,

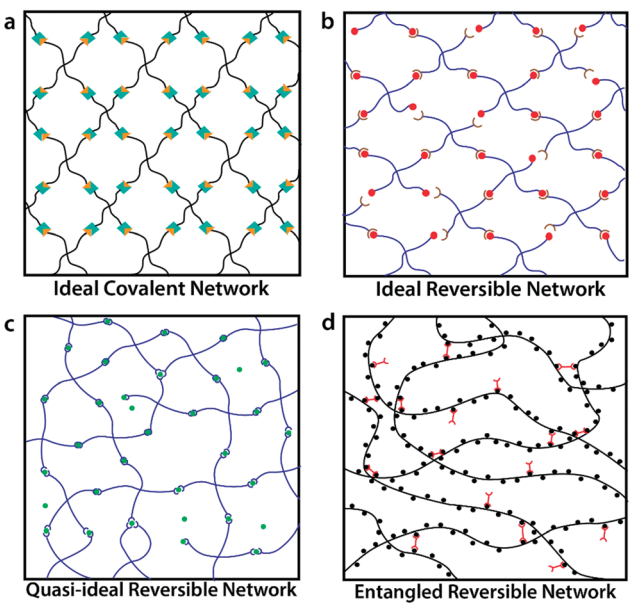

Fig. 1 Schematics of (a) ideal covalent polymer network, featuring well-controlled network structure and permanent crosslinks;[1,2] (b) the proposed ideal reversible polymer network, featuring well-controlled network structure and reversible crosslinks; (c) quasi-ideal reversible polymer network,[3,4] with reversible crosslinks but possibility of local defects and loops; and (d) entangled reversible polymer network,[5,6] with reversible crosslinks and chain entanglements.

[a] *Dept. of Chemical Engineering, MIT, 77 Massachusetts Ave., Cambridge, MA, USA*
[b] *Soft Active Materials Laboratory, Dept. of Mechanical Engineering, MIT, 77 Massachusetts Ave., Cambridge, MA, USA. E-mail: zhaox@mit.edu*
[c] *Dept. of Civil and Environmental Engineering, MIT, 77 Massachusetts Ave., Cambridge, MA, USA*

electrostatic and hydrophobic interactions, and host–guest domains,[15–18] have been extensively studied to design materials featuring self-healing properties,[19,20] controlled stress–relaxations,[21,22] bio-inspired adhesive behavior,[3,23] and high fracture toughness.[24] Existing studies on reversible crosslinks are mostly based on measurements and modeling of single molecules,[25,26] reversible crosslinks on membranes[27,28] or reversible crosslinks in random polymer networks.[3,5,29–32] Well-controlled polymer networks containing reversible crosslinks (as shown in Fig. 1b) could facilitate better understanding of the reversible crosslinks themselves, and provide better controls over the physical properties of resultant networks. However, such well-controlled polymer networks with reversible crosslinks have rarely been synthesized or studied.[33–35] Non-ideal networks are ubiquitous in the literature. For instance, researchers at the Holten-Andersen group have used 4-arm polyethylene glycol (PEG) containing metal–ligand coordination moieties (pyridine and catechol) at the chain ends.[23,36,37] Upon the addition of metal ions, the PEG molecules are crosslinked to generate quasi-ideal reversible polymer networks with locally uncontrolled structures due to self-crosslinking between arms of the same macromer and crosslinking of more than two arms on the same metal ion (shown in Fig. 1c). As another example, researchers at the Craig group have synthesized and characterized dimethyl sulfoxide-based poly-4-vinylpyridine (PVP) networks crosslinked by small pincer-like bifunctional molecules with metal–ligand groups at the ends. Given the high molecular weight of PVP used, these networks contain chain entanglements (shown in Fig. 1d).[5,6,38]

In this article we introduce the concept of ideal reversible polymer networks, which have well-controlled polymer network architectures similar to their covalent counterparts but feature reversible crosslinks (Fig. 1b). Unlike the entangled and quasi-ideal networks,[3,39–41] there are no entanglements, other topological defects or point defects (crosslinks with different functionality) in these ideal reversible networks. Moreover, the networks exhibit time-dependent mechanical properties (*i.e.* viscoelasticity), due to the association and dissociation of the reversible crosslinks in them. We formulate a theoretical framework to quantitatively correlate the viscoelastic responses with the network architecture and properties of the reversible crosslinks. In this theory, the ideal reversible polymer networks are constituted of small end-functionalized 4-arm macromers near the overlap concentration, of which half are functionalized with group A and half with group B. All arms of the macromers are non-entangled (below critical entanglement molecular weight) and of equal length. Functional groups A and B are complementary and can form reversible crosslinks with each other but not with themselves. At equilibrium, a pair of complementary groups can be either at the unbound state (A + B) or the bound state C, which corresponds to a crosslink in the network (Fig. 2a).[28] In the current theory, we use the Bell model[28] to characterize the association and dissociation of the complementary reversible crosslinks. The theory can also be extended to incorporate other models for dynamics of reversible crosslinks such as the Evans model.[42,43]

Consequently, the theory gives that the ideal reversible polymer networks possess the following time-dependent mechanical properties: (i) their viscoelasticity resembles a single Maxwell element with a spring and a dashpot in series, (ii) the equilibrium concentration of bound reversible crosslinks determines the instantaneous shear modulus of the Maxwell element, and (iii) the time scale for dissociation of the crosslinks determines the relaxation time of the Maxwell element. Only a single relaxation time is expected for the ideal reversible networks due to the absence of intra-chain or inter-chain entanglements (low molecular weight macromers near the overlap concentration), and the fact that any Rouse relaxation process will occur much faster than the dissociation of reversible crosslinks.

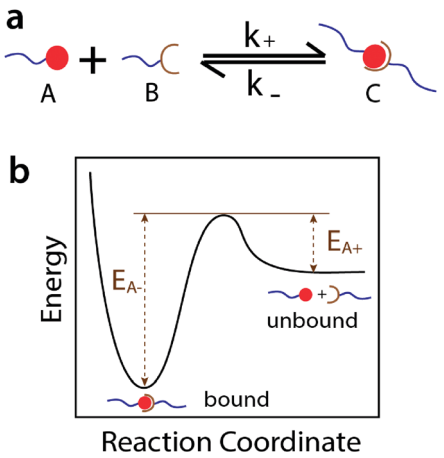

Fig. 2 (a) Reversible crosslinks feature a reversible reaction of functional groups A and B with association rate k_+ and dissociation rate k_-. (b) Energy landscape of the reversible reaction, with activation energies E_{A+} and E_{A-} for the forward and reverse reactions, respectively.

Based on this theory, we further develop a set of general methods: (i) to independently control the instantaneous shear modulus and relaxation time of ideal reversible networks by independently varying the equilibrium concentration of crosslinks and dissociation time, respectively; and (ii) to quantitatively derive the kinetic parameters of the reversible crosslinks including reaction rates and activation energies from macroscopic measurements of viscoelastic properties of the ideal reversible polymer networks.

In order to validate the theory and methods proposed, we synthesized and characterized a hydrogel composed of 4-arm polyethylene glycol polymers end-functionalized with 3-fluorophenylboronic acid groups (*i.e.*, group A) and diol groups (*i.e.*, group B), respectively.[33] The phenylboronic acid–diol reversible reaction is sensitive to pH and temperature, which can be varied to tune the kinetics of the reversible reaction.[44–47] The 4-arm macromers with two different end-groups were mixed at equimolar ratio to form polymer networks around the overlap concentration of the macromers. The hydrogels were subjected to stress relaxation and small amplitude oscillatory shear tests in a rheometer to characterize its mechanical responses. All tests yielded viscoelastic behaviors of the reversible network equivalent to a Maxwell element, as predicted by the theory. The proposed method to independently control viscoelastic properties of ideal polymer networks were also validated experimentally. The concentrations of macromers were

changed to control instantaneous shear modulus, while temperature and pH were varied to control both instantaneous shear modulus and relaxation time. The resultant changes of the network's viscoelastic properties quantitatively followed our theory's prediction. We further calculated the kinetic parameters of reversible crosslinks including reaction rates and activation energies from experimentally measured viscoelastic properties of the networks. The resultant values were consistent with previously-reported values.

Through a combination of theory and experiments, the current work not only lays the theoretical foundation for ideal reversible polymer network but also provide simple yet general methods to quantitatively control viscoelasticity of polymer networks (without the involvement of entanglements) and to measure kinetic properties of reversible crosslinks based on macroscopic mechanical properties. While reversible crosslinks have been widely used in the design of hydrogels with extraordinary mechanical properties[24,48–51] and hydrogel-based biomedical devices,[52–55] we expect the current work will provide better understanding and control of reversible crosslinks and polymer networks.[3,11,36,56–61] In addition, the current study may shed light on how reversible polymer networks are controlled in biological systems.[15,17,21,62,63]

Theory of ideal reversible polymer networks

Kinetics of reversible crosslinks

The overall association and dissociation of two complementary functional groups (schematically illustrated in Fig. 2a) can be expressed as

$$\mathrm{A} + \mathrm{B} \underset{k_-}{\overset{k_+}{\rightleftharpoons}} \mathrm{C} \tag{1}$$

where k_+ and k_- are the rates for association and dissociation of the reversible crosslink, respectively. The equilibrium constant of the reaction is defined as $K = k_+/k_-$. It is common to assume that the kinetics of reversible crosslinks are reaction-limited (*i.e.*, the diffusion rates of functional groups are much higher than the rates for forward and reverse reaction of the encounter complex).[3,11,28,56,59,64,65] Therefore, the association and dissociation rates of the reversible crosslink (k_+ and k_-) are determined by the forward and reverse reaction rates, which can be expressed based on the transition state theory and Arrhenius equation as

$$k_+ = k_{0+}\exp\left(\frac{-E_{\mathrm{A}+}}{k_{\mathrm{B}}T}\right) \tag{2a}$$

$$k_- = k_{0-}\exp\left(\frac{-E_{\mathrm{A}-}}{k_{\mathrm{B}}T}\right) \tag{2b}$$

where $k_{\mathrm{B}}T$ is the thermal energy scale (Boltzmann constant times absolute temperature), $E_{\mathrm{A}+}$ is the activation energy (energy barrier) and k_{0+} is the pre-exponential factor for the forward reaction, and $E_{\mathrm{A}-}$ and k_{0-} are the corresponding parameters for the reverse reaction. When mechanical force is applied on the bond, the energy landscape is assumed to be altered such that the activation energy for the reverse reaction decreases proportionally to the force applied,[28]

$$k_- = k_{0-}\exp\left(\frac{-(E_{\mathrm{A}-} - \gamma f)}{k_{\mathrm{B}}T}\right) \tag{3}$$

with a bond-specific proportionality parameter γ. If the applied deformation on the reversible polymer network is relatively small, the resultant γf can be much lower than $E_{\mathrm{A}-}$ and thus the effect of applied force f on the dissociation rate is negligible.

Concentration of reversible crosslinks at equilibrium

Let N_{A} and N_{B} be the number of functional groups A and B (at unbound and bound states) per unit volume of the polymer network, respectively; and N_{C} the number of crosslinks (bound state) per unit volume of the polymer network. N_{A}, N_{B} and N_{C} are also the concentrations of the corresponding functional groups and crosslinks. The formation of the crosslinks is assumed to follow the following kinetic equation,[28]

$$\frac{\mathrm{d}N_{\mathrm{C}}}{\mathrm{d}t} = k_+(N_{\mathrm{A}} - N_{\mathrm{C}})(N_{\mathrm{B}} - N_{\mathrm{C}}) - k_-N_{\mathrm{C}} \tag{4}$$

At equilibrium $\mathrm{d}N_{\mathrm{C}}/\mathrm{d}t = 0$. Then N_{C} is given by

$$N_{\mathrm{C}} = \frac{1}{2}\left(N_{\mathrm{A}} + N_{\mathrm{B}} + \frac{1}{K}\right) - \frac{1}{2}\left[\left(N_{\mathrm{A}} + N_{\mathrm{B}} + \frac{1}{K}\right)^2 - 4N_{\mathrm{A}}N_{\mathrm{B}}\right]^{1/2} \tag{5}$$

where K is the equilibrium constant of the reaction. In the current model $N_{\mathrm{A}} = N_{\mathrm{B}}$ (*i.e.* A and B mixed at equimolar amounts). The conversion of functional group A is defined as $p = N_{\mathrm{C}}/N_{\mathrm{A}}$, which is equivalent to the conversion of group B. Based on eqn (5), the conversion can be expressed as

$$p = \left(1 + \frac{1}{2N_{\mathrm{A}}K}\right) - \left[\left(1 + \frac{1}{2N_{\mathrm{A}}K}\right)^2 - 1\right]^{1/2} \tag{6}$$

Concentration of elastically-active chains at equilibrium

The formation of a crosslink does not guarantee the formation of an elastically-active chain in the ideal reversible polymer network as illustrated in Fig. 3a. If only one arm of the macromer is crosslinked to the network, this macromer is a dangling end and does not contribute to the network's elasticity. If two arms are crosslinked to the network, the macromer will either act as a loop or a bridging chain, neither of which contribute to the network's elasticity. Only when 3 or 4 arms are crosslinked to the network the macromer will become elastically-active and contribute to the network's elasticity. The probabilities for a macromers to have three (P_3) or four (P_4) arms crosslinked to the infinite network are functions of the conversion p[66]

$$P_3 = 4P_{\mathrm{out}}(1 - P_{\mathrm{out}})^3 \tag{7a}$$

$$P_4 = (1 - P_{\mathrm{out}})^4 \tag{7b}$$

where $P_{\mathrm{out}} = \sqrt{1/p - 3/4} - 1/2$ is the probability for a crosslink to lead to a dangling chain.[66] Since it is not possible to achieve a percolated network when P_{out} is equal or greater than

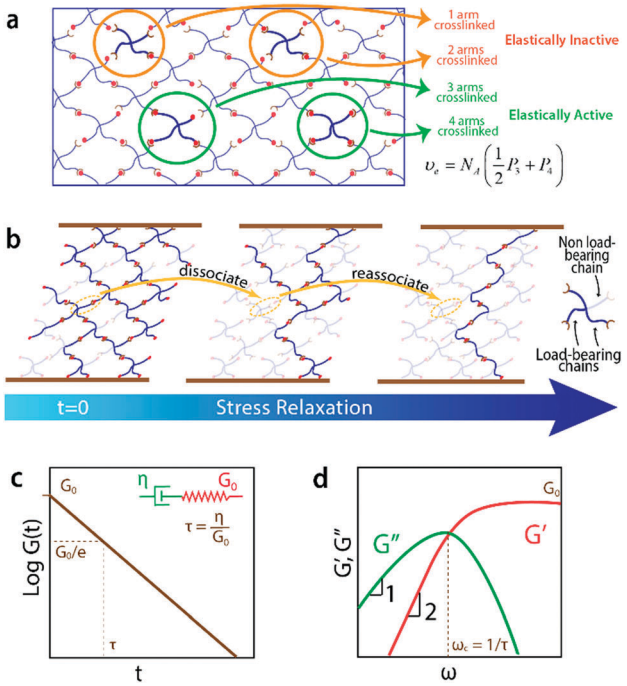

Fig. 3 (a) Only macromers with three or four arms crosslinked to the network are elastically-active upon network deformation. The concentration of elastically-active chains, υ_e, is given by a weighted sum of the concentrations of macromers with three or four arms crosslinked at equilibrium. (b) When subjected to stress at t = 0, the concentration of load-bearing chains, υ_e^{load}, decreases with time as the dissociated chains relax and do not bear the initial load, even if they re-associate. (c) Stress relaxation curve for a Maxwell model, with a single relaxation time τ and instantaneous modulus G_0. (d) Dynamic moduli curves for a Maxwell element from small amplitude oscillatory rheology, with expected scaling regimes and crossover frequency ω_c.

one, there is a threshold for the minimum value of conversion p_{min} = 1/3 under which it is not possible to form a network. From eqn (6), we can further derive the condition to form a percolated network as $N_A K > 0.75$.

The concentration of elastically-active chains at equilibrium, υ_e, is then given by a weighted sum of the concentrations of macromers with 3 and 4 crosslinked arms. Specifically, macromers with 4 crosslinked arms contribute 4 elastically-active chains (one per arm) while those macromers with 3 crosslinked arms contribute 1.5 elastically-active chains (one half per arm), as described by Langley and Polmanteer.[66,67]

Therefore υ_e can be expressed as

$$\upsilon_e = N_A\left(\frac{3}{2}P_3 + 4P_4\right) = \frac{N_A}{8}\left(3 - \sqrt{\frac{4}{p} - 3}\right)^3\left(3 + \sqrt{\frac{4}{p} - 3}\right) = \frac{N_C}{8p}\left(3 - \sqrt{\frac{4}{p} - 3}\right)^3\left(3 + \sqrt{\frac{4}{p} - 3}\right) \quad (8)$$

When a network is formed, both N_A and K are determined and thus the equilibrium conversion p is fixed. From the equation above it can be seen that υ_e is linearly related with the N_C when conversion p is a constant.

Concentration of loading-bearing chains during stress relaxation test

Let's imagine we carry out a stress relaxation test on the ideal reversible polymer network by applying a constant shear strain of small magnitudeεon the network beginning at time t = 0 and measuring the resulting shear stress $\sigma(t)$ over time. The stress–relaxation shear modulus of the network is defined as,

$$G(t) = \frac{\sigma(t)}{\varepsilon} \quad (9)$$

Assuming affine deformation of the polymer network, the instantaneous shear modulus $G_0 = G(t = 0)$ of the network can be calculated as

$$G_0 = \upsilon_e k_B T \quad (10)$$

As time evolves ($t > 0$), some of the elastically-active chains that carry load will dissociate and thus reduce the shear modulus of the network from G_0 to $G(t)$. While new crosslinks and new elastically-active chains can form in the network, these newly-formed chains will not carry the load initially applied (Fig. 3b). Let's denote the number of load-bearing chains and load-bearing crosslinks per unit volume of the network as υ_e^{load} and N_C^{load}, respectively. Assuming affine deformation of the load-bearing chains over time, we can express $G(t)$ as,

$$G(t) = \upsilon_e^{load} k_B T \quad (11)$$

Since the applied strain is small, we assume the force applied to load-bearing crosslinks does not affect the energy landscape of the crosslink nor its reverse rate constant (k_-). Therefore, the kinetic equation for N_C^{load} during the stress relaxation test is,

$$\frac{dN_C^{load}}{dt} = -k_- N_C^{load} \quad (12)$$

In addition, υ_e^{load} and N_C^{load} are linearly related with each other, per eqn (8), as the stress relaxation test has no effect on the conversion. Therefore, we can further express the kinetic equation for υ_e^{load} during stress relaxation test as,

$$\frac{d\upsilon_e^{load}}{dt} = -k_- \upsilon_e^{load} \quad (13)$$

Maxwell model of ideal reversible polymer networks

By solving eqn (13) with the initial condition $\upsilon_e^{load}(t = 0) = \upsilon_e$, we can calculate the evolution of the concentration of load-bearing chains in an ideal reversible polymer network during stress relaxation test as

$$\upsilon_e^{load}(t) = \upsilon_e \exp(-k_- t) \quad (14)$$

By substituting eqn (14) into eqn (11), the stress–relaxation shear modulus of the network is given by,

$$G(t) = \upsilon_e k_B T \exp(-k_- t) \quad (15)$$

From eqn (15), it can be seen that the ideal reversible polymer network behaves as a Maxwell element with instantaneous

shear modulus $G_0 = \upsilon_e k_B T$ and relaxation time constant $\tau = 1/k_-$ during a stress relaxation test (Fig. 3c). As a linear viscoelastic material, the ideal reversible polymer network should follow the Maxwell model in other modes of small deformations as well. For example, if the ideal reversible polymer network undergoes a small-amplitude oscillatory shear test with frequency ω, the measured storage modulus G' and loss modulus G'' should follow the equations of a Maxwell model (Fig. 3d),

$$G' = \upsilon_e k_B T \frac{\omega^2}{\omega^2 + (k_-)^2} \tag{16a}$$

$$G'' = \upsilon_e k_B T \frac{\omega k_-}{\omega^2 + (k_-)^2} \tag{16b}$$

These results show that the ideal reversible polymer networks have identical mechanical responses as the transient polymer network model at the Green–Tobolosky limit.[30,68] This convergence is not surprising since both models assume a single mechanism for stress relaxation, a constant dissociation rate of crosslinks at experimental timescales and affine deformation of elastically-active chains. Given the well-defined nature of the ideal reversible polymer networks, the theory is able to explain the physical origins of G_0 and τ, and provide equations to predict their values based on physical parameters of the network and reversible crosslinks in a quantitative way.

Methods to control instantaneous shear modulus and relaxation time

The developed theory provides guidelines to tune the instantaneous shear modulus G_0 and the relaxation time τ of an ideal reversible polymer network independently, as G_0 and τ arise from different physical mechanisms. Here we outline a set of methods to independently control instantaneous shear modulus and relaxation time.

The instantaneous shear modulus of the network is solely controlled by the equilibrium concentration of elastically-active chains υ_e. By combining eqn (6), (8) and (11), it is possible to obtain an explicit but complex expression relating υ_e to the equilibrium constant K and concentration of functional group A, N_A,

$$G_0/k_B T = \frac{N_A}{16}\left(3 - \sqrt{\frac{4}{p} - 3}\right)^3 \left(\sqrt{\frac{4}{p} - 3} + 1\right) \tag{17}$$

where p is a function of N_A and K per eqn (6). Since the concentration of total 4-arm macromers equals $N_A/2$, eqn (17) also relates the instantaneous shear modulus with macromer concentration. In Fig. 4a, we plot $G_0/k_B T$ *vs.* N_A for various values of K. The range of N_A in Fig. 4a corresponds to typical concentrations of macromers near the overlap concentration.[69] The relation of G_0 and N_A across the chosen range can be captured by the following scaling relation,

$$G_0 \sim (N_A)^m \tag{18}$$

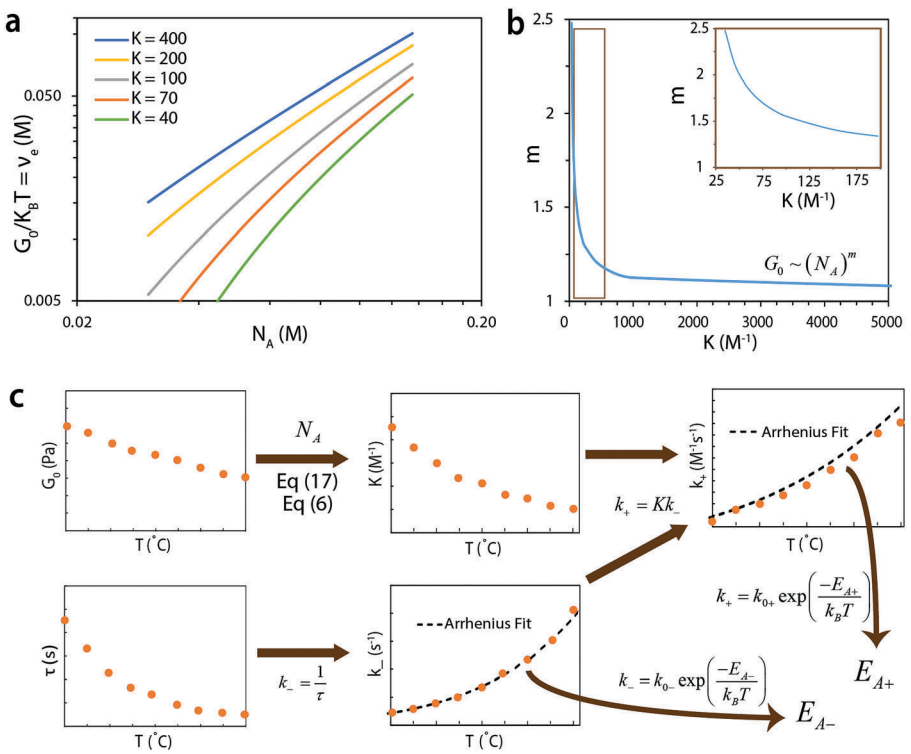

Fig. 4 (a) Predicted relations of $G_0/k_B T$ *vs.* N_A for different equilibrium constants. (b) G_0 scales with N_A following a power law with exponent m, which depends on equilibrium constant K. (c) The values of G_0 at different temperatures and known N_A can be used to determine K at the corresponding temperatures. The values of τ at different temperatures can be used to determine k_-. With K and k_-, one can further calculate k_+. Fitting the curves of k_- *vs.* T and k_+ *vs.* T to Arrhenius relations yields the corresponding activation energies.

where the scaling exponent m is a function of K (shown in Fig. 4b). When $K \to \infty$, $m \to 1$, which indicates that when all reversible crosslink are in the bound state, G_0 is linearly related to N_A. This limiting case is equivalent to the ideal covalent network model. As shown in the inset of Fig. 4b, m ranges from 1.5 to 2.5, when K ranges from 25–200. Since m is positive, increasing the macromer concentration will yield an increase in G_0. From eqn (18), it is clear that G_0 can be tuned with the following three methods:

Method 1 to control G_0: with fixed macromer concentration, one can change the functional groups A and B on the macromers or the conditions of the network (*e.g.*, temperature, pH) to change the equilibrium constant K and thus vary both the scaling component m and instantaneous shear modulus G_0. Note that this method will also vary the relaxation time of the network, which will be discussed in the next section of the paper.

Method 2 to control G_0: with fixed equilibrium constant K, one can directly vary the macromer concentration near the overlap concentration to tune G_0. This strategy will not vary the relaxation time of the network. However, the range of tunable G_0 is relatively limited in this strategy since the macromer concentration needs to be around overlap concentration.

Method 3 to control G_0: for a fixed equilibrium constant K, one can change the molecular weight of the macromer M while maintaining the macromers at the overlap concentration. The pervaded volume of a macromer V scales with the macromer molecular weight by $V \propto M^{3\upsilon}$, where υ is a scaling exponent that depends on the solvent quality. The value of υ is approximately 0.6 for polymers in a good solvent, such as PEG in aqueous solution.[69] Furthermore, at the overlap concentration, the macromer concentration and macromer pervaded volume scales as $N_A \propto V^{-1}$. Therefore, we can obtain a scaling between instantaneous shear modulus G_0 and macromer molecular weight M at the overlap concentration,

$$G_0 \sim M^{-3\upsilon m} \tag{19}$$

Compared with Method 2, this method can give a larger tunable range for G_0, since the molecular weight of the macromers can varied significantly (up to the entanglement molecular weight). Furthermore, similar to method 2, changing M will not vary the relaxation time of the network.

From the theory section, the relaxation time τ for the reversible network is only determined by the dissociation rate of the reversible crosslink, k_-. Therefore, we can use the following strategy to tune τ. One can change the functional groups A and B or the network conditions (*e.g.*, temperature, pH) to vary k_- and thus vary τ, since $\tau = 1/k_-$. It is important to note that adjusting k_- will change K, so the scaling component m and instantaneous shear modulus G_0 will also change. Therefore, to maintain G_0 constant while tuning τ, it is necessary to vary the macromer concentration and/or molecular weight accordingly.

The methods to control G_0 and τ introduced here are general for all ideal reversible network regardless of the reversible bond type used. For quasi-ideal and entangled networks, such as those systems used in past literature,[3,4,31,32,36,56,58,59] the methods will be applicable in a qualitative way only.

Method to measure kinetic parameters of reversible crosslink from macroscale mechanical tests

The theory of ideal reversible network further allows one to quantitatively measure the kinetic parameters of reversible crosslink including association and dissociation rates (k_+, k_-) and activation energies for forward and reverse reactions (E_{A+}, E_{A-}) from macroscale mechanical tests of the network (*i.e.* G_0 and τ data).

For a given ideal reversible polymer network in an aqueous environment, the macromer concentration $N_A/2$ and network parameters such as temperature T are known. From the stress relaxation test or the small-amplitude oscillatory shear test, we can measure G_0 and τ at various temperatures. From the measured τ, we can calculate the dissociation rate $k_- = 1/\tau$ at various temperatures. Then, by fitting eqn (2b) to the curve of k_- *vs.* T, we can obtain the activation energy for reverse reaction E_{A-}.

On the other hand, from the macromer concentration we can determine N_A. This can be used with G_0 values at various temperatures to calculate K at the corresponding temperatures through eqn (6) and (17). Since k_- at various temperatures are known, we can calculate the corresponding association rates $k_+ = Kk_-$. Thereafter, by fitting eqn (2a) to the curve of k_+ *vs.* T, we can obtain activation energy for forward reaction E_{A+}.

Materials and methods

To validate the theory of ideal reversible polymer network and the consequent methods to tune and measure properties of the network, we have selected, synthesized and studied a model hydrogel system.

In this work, we chose a 4-arm PEG-based reversible hydrogel system analogous to the 4-arm PEG-based ideal covalent networks developed by Sakai, Shibayama and colleagues.[1,2,9,10] These networks contained very low amounts of entanglements and defects since the macromers behave as space-filling blobs that form a regular percolated network around the overlap concentration.[1] To implement reversible crosslinking, we introduced 3-fluorophenylboronic acid functional groups (*i.e.*, A group) and diol functional groups (*i.e.*, B group) to the PEG macromers (Fig. 5). The dynamic covalent phenylboronic acid–diol chemistry was selected due to ease of synthesis, detailed molecular understanding of bonding kinetics and ability to tune the bonding kinetics by changing pH, temperature or the substituents on the phenyl ring.[44–47,70] While this reaction was not strictly bimolecular,

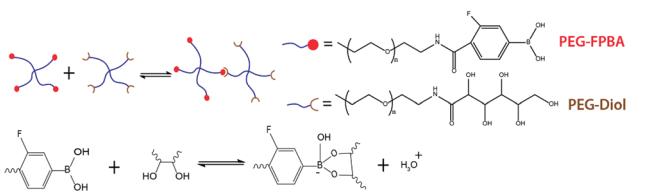

Fig. 5 Chemical structure of the reversible crosslink. Two end-functionalized 4-arm PEG molecules bond reversibly through phenylboronic acid–diol complexation chemistry, which is highly specific, reversible at experimental timescales, and sensitive to pH and temperature.

we used the conditional (or effective) formation constant framework to account for the effects of pH on the reversible reaction.[46] Then, the reversible crosslinking could be described as a single reaction with unique equilibrium constant, forward and reverse rate constants (K, k_+ and k_-, respectively) at a fixed pH.

The functionalized PEG components were synthesized following the protocol published by Yesilyurt *et al.*[33] Briefly, amino-terminated 4-arm PEG (5k or 10k, Jenkem Technologies) was conjugated to either D-gluconolactone or 4-carboxy-3-fluorophenylboronic acid (Sigma). The purified PEG-Diol and PEG-FPBA products were freeze-dried and stored at −20 °C until use. Separate PEG-Diol and PEG-FPBA solutions (with concentrations ranging from 15 to 25 mM) were made in 1× PBS buffer (pH 7.5, adjusted with 1 M NaOH). Additional amounts of 0.1 M NaOH were added to each solution to control the final pH of the hydrogel. The final pH was estimated using the Henderson–Hasselbalch equation with knowledge FBPA's pK_a (7.2).[33] The hydrogels were synthesized by mixing equal amounts of the PEG macromer solutions.

The mechanical properties of the model hydrogels were measured with a controlled stress rheometer AR-G2 (TA Instruments, New Castles, DE) fitted with a Peltier plate and a 20 mm 4° steel cone fixture. The PEG-Diol and PEG-FPBA solutions (100 μL of each) were directly mixed in the rheometer bottom plate and a solvent trap was used to prevent dehydration. The samples were equilibrated for 5 min prior to testing. The linear viscoelasticity region was determined by oscillatory strain amplitude sweeps at 1 Hz. This region extended up to 20% strain. Oscillatory frequency sweeps were conducted at 2% strain amplitude in the 0.1–100 rad s^{-1} range, 10 points per decade. Stress relaxation tests were carried out for 3 or 6 minutes at a constant strain of 10%. Analysis and fitting of the data was carried out using built-in non-linear fitting algorithms in OriginPro 8.5, and plotting was done with Microsoft Excel.

Results and discussion

To validate the theory of ideal reversible polymer networks, we carried out a set of stress relaxation and small-amplitude oscillatory shear tests on reversibly crosslinked 4-arm PEG networks at various temperatures (from 5 °C to 45 °C) and pH values (from 6.9 to 8.1). The molecular weight of the macromers was 5000 g mol^{-1} and they were at a total concentration of 15 mM in aqueous solution.

The relaxation shear moduli $G(t)$ measured for hydrogels at pH of 7.20 and various temperatures as functions of time t was plotted in Fig. 6a (on a semi-log plot). The curves indicated that the 4-arm PEG reversible network at each temperature indeed behaved as a Maxwell element with a defined instantaneous shear modulus and a single relaxation time, as demonstrated by the single slope.

In principle it is possible to have additional relaxation mechanisms in a polymer network such as entanglements or Rouse-type modes of relaxation.[69,71] As shown by Sakai and colleagues,[1,2,10] entanglements can be avoided by using small 4-arm macromers near the overlap concentration. As for Rouse chain relaxation, the longest relaxation timescale is given by $\tau_1 \sim \tau_{seg}N^2$, where N is the number of Kuhn monomers in the chain and τ_{seg} is the relaxation time of a single Kuhn monomer.[69,71] Since the macromers used in this work have low molecular weight (5000 g mol^{-1}), the Rouse relaxation times ($\sim 10^{-6}$–10^{-4} s) are at least three orders of magnitude below the reversible crosslink relaxation times,[72] and won't be observed in these experiments.

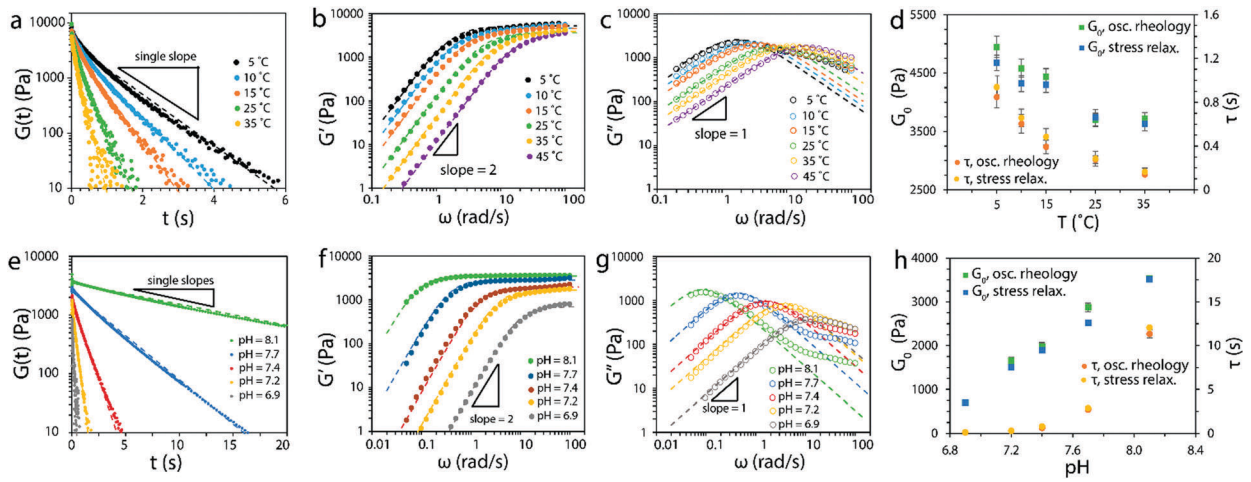

Fig. 6 (a) Relaxation shear moduli, (b) storage moduli and (c) loss moduli of the 4-arm PEG reversible networks at pH = 7.2 and various temperatures. Non-linear fittings to eqn (15), (16a) and (16b) are shown as dashed lines. (d) Comparison of G_0 and τ values obtained from oscillatory rheology and stress relaxation at pH = 7.2 and various temperatures. (e) Relaxation shear moduli, (f) storage moduli and (g) loss moduli of the 4-arm PEG reversible networks at T = 25 °C and various pH values. Non-linear fittings to eqn (15), (16a) and (16b) are shown as dashed lines. (g) Comparison of G_0 and τ values obtained from oscillatory rheology and stress relaxation at T = 25 °C and various pH values. The molecular weight of the macromers used was 5000 g mol^{-1} and the total concentration was 15 mM.

The storage moduli $G'(\omega)$ and loss moduli $G''(\omega)$ measured at various temperatures as functions of frequency ω are plotted in Fig. 6b and c. The curves obtained at various temperatures were fitted to the Maxwell model eqn (15), (16a) and (16b) and plotted as dashed lines. The fitting was adequate and showed the expected scaling as a function of ω, that is, $G' \sim \omega^2$ and $G'' \sim \omega$ up to the crossover frequency. Deviations on the $G''(\omega)$ curve were seen at high frequencies, observation that will be discussed in the next paragraph. In addition, the instantaneous shear modulus G_0 and relaxation time$\tau$of the network obtained from two different tests (stress relaxation and oscillatory rheology) at the same temperature were consistent with each other (Fig. 6d).

Similarly, the measurements of the 4-arm PEG reversible network at 25 °C and various pH values indicated the network followed the Maxwell model (Fig. 6e–g) up to the crossover frequency (deviations in $G''(\omega)$ were also present). The measured values of instantaneous shear modulus G_0 and relaxation time τ from the two tests at the same pH were also consistent with each other (Fig. 6h). The results shown in Fig. 6a–h validated the prediction of our theory that ideal reversible polymer networks at various temperatures and pH values have Maxwell-like mechanical responses (the deviations seen at high frequencies will be discussed below). In addition, the results showed that the instantaneous shear moduli G_0 and relaxation timeτ of the network can be tuned by varying the temperature and pH of the network.

The proposed ideal reversible polymer network theory assumes the association and dissociation of crosslinks takes place at experimental timescales. Therefore the model proposed is applicable when the experimental timescale $t_{exp} \sim 1/\omega$ is greater or equal than the dissociation timescale τ. When the network is tested in a regime in which $t_{exp} \ll \tau$, the reversible crosslinks cannot dissociate so the network will resemble a covalently-crosslinked network, characterized by no stress relaxation and G' and G'' independent of ω. The effect of these two different regimes in rheology experiments is that the networks will exhibit Maxwell behavior up to frequencies near the crossover frequency $\omega_c = 1/\tau$, and will transition to the covalent-like regime for frequencies above. The deviations from a Maxwell behavior seen in Fig. 6c and g at high frequencies arose from such transition, as the G'' curve will plateau to match the scaling at the covalent-like regime. No transition was observed in the G' curves as the plateau scaling is already realized.

In order to validate that the proposed methods can control mechanical properties of reversible networks and measure kinetic parameters of reversible crosslinks, we systematically varied the concentration and molecular weight of the 4-arm PEG, the temperature and pH of the network. We then measured G_0 and τ for the resultant networks *via* stress relaxation and small amplitude oscillatory shear rheology tests. In Fig. 7a, we plotted the instantaneous shear moduli G_0 of 4-arm PEG reversible networks with macromer molecular weight of 5k at an estimated pH of 7.2 as functions of macromer concentration and temperature. It is evident that both varying macromer concentration and temperature could be used to tune G_0. In Fig. 7b, we further plotted the relaxation time values of the same set of reversible networks. While τ could be tuned by changing temperature, it could not be significantly tuned by macromer concentration at the same temperature since the properties of reversible crosslinks are not affected by changing macromer concentration alone. These results validated that the mechanical properties of reversible networks can be controlled according to the methods proposed in this work.

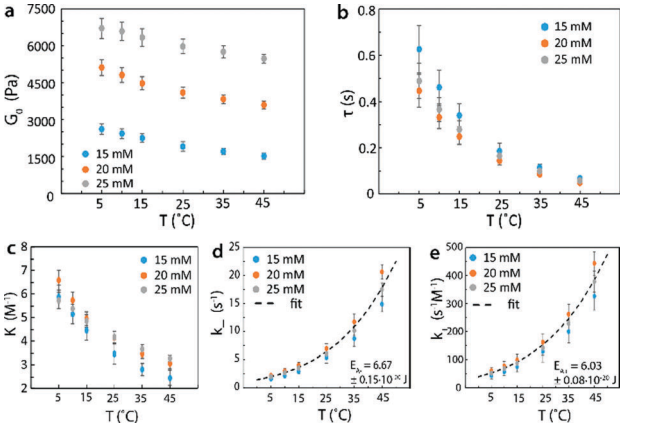

Fig. 7 (a) Instantaneous shear moduli of 4-arm PEG reversible network at different macromer concentrations and temperatures. (b) Relaxation times of 4-arm PEG reversible network at different macromer concentrations and temperatures. (c) Equilibrium constants at different macromer concentrations and temperatures. (d) Dissociation rate of the reversible crosslink at different macromer concentrations and temperatures with Arrhenius fit to give the activation energy. (e) Association rate of the reversible crosslink at different macromer concentrations and temperatures with Arrhenius fit to give the activation energy. The molecular weight of the macromers used was 5000 g mol^{-1} and the network pH was 7.2.

In addition, G_0 was proportional to the concentration of elastically-active chains υ_e (per eqn (10)). With the known υ_e and the functional group concentration N_A, eqn (6) and (17) were solved to determine the equilibrium constants K at every temperature [Fig. 7c]. The measured relaxation time τ further gave the dissociation rates at every temperature, since $k_- = 1/\tau$ (Fig. 7d). Then, the association rates of reversible crosslink at various temperatures were calculated as $k_+ = Kk_-$ (Fig. 7e). It is noted that the measured K, k_- and k_+ for 4-arm PEG reversible networks did not depend on macromer concentration, as predicted by the theory. By fitting the k_+ and k_- curves to eqn (2a) and (2b), we obtained the activation energies for forward and reverse reactions of the reversible crosslink, respectively. For this network, the values were $E_{A+} = 6.03 \pm 0.08 \times 10^{-20}$ J and $E_{A-} = 6.67 \pm 0.15 \times 10^{-20}$ J. These values indicate that the forward reaction was more energetically favorable (with lower activation energy) at pH = 7.2, which led to the formation of a crosslinked network. The kinetic parameters of the reversible crosslink measured by our proposed method were in the same range as published activation energy values (note that the reported numbers are for different boronic acid and diol species).[73,74]

In Fig. 8, we repeated the process with identical 4-arm PEG reversible networks at a higher pH of 7.7. It can be seen that the trends of G_0 and τ *vs.* temperature measured at this higher pH value (Fig. 8a and b) were the same as those measured at

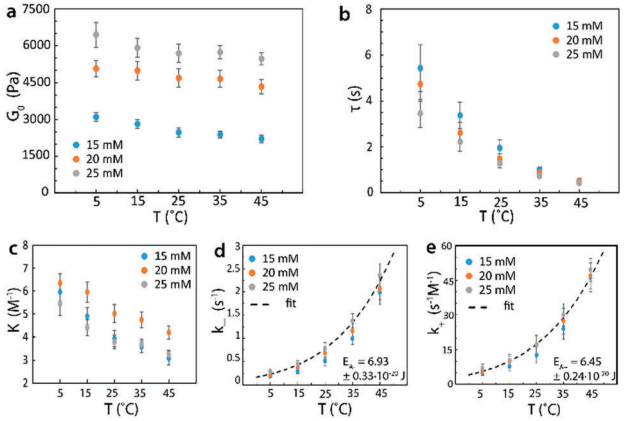

Fig. 8 (a) Instantaneous shear moduli of 4-arm PEG reversible network at different macromer concentrations and temperatures. (b) Relaxation times of 4-arm PEG reversible network at different macromer concentrations and temperatures. (c) Equilibrium constants at different macromer concentrations and temperatures. (d) Dissociation rate of the reversible crosslink at different macromer concentrations and temperatures with Arrhenius fit to give the activation energy. (e) Association rate of the reversible crosslink at different macromer concentrations and temperatures with Arrhenius fit to give the activation energy. The macromers' molecular weight was 5000 g mol^{-1} and the network pH was 7.7.

pH = 7.2 (Fig. 7a and b). However, at the same temperature, values for G_0 and τ at pH = 7.7 were higher than the corresponding values pH = 7.2, as increasing pH leads to lower dissociation rates and higher equilibrium constants for the phenylboronic acid–diol reversible reaction.[44–47] These results were consistent with our theory's predictions, and validated that changing pH can also be used to tune G_0 and τ of reversible networks. In addition, from the mechanical properties of reversible network, we could again determine the activation energies. These values were $E_{A+} = 6.45 \pm 0.24 \times 10^{-20}$ J for the forward reaction and $E_{A-} = 6.93 \pm 0.33 \times 10^{-20}$ J for the reverse one. These values were also in the same range as the published values and higher than the values measured at pH 7.2.

Conclusions

This work introduced ideal reversible polymer networks, defined as networks crosslinked by reversible junctions that would revert to ideal covalent polymer networks if all reversible junctions were replaced by covalent bonds. Through a combination of theory and experiments, we showed that the viscoelasticity of ideal reversible polymer network follows the Maxwell model, characterized by instantaneous shear modulus G_0 and relaxation time τ. The value of G_0 for ideal covalent polymer networks can be tuned by varying concentration and molecular weight of the macromers and pH and temperature of the aqueous solution of the network. The relaxation time τ is controlled by pH and temperature of the aqueous solution of the network, but not concentration or molecular weight of the macromers. These results not only lay the theoretical foundation for ideal reversible polymer network but also provide simple yet general methods to quantitatively control viscoelasticity of polymer networks and to measure kinetic properties of reversible crosslinks based on their viscoelasticity. We expect the current work will facilitate the design of polymer networks to achieve extraordinary properties *via* reversible crosslinks and the understanding of reversible polymer networks in various synthetic and biological polymers.

Conflicts of interest

There are no conflicts to declare.

Acknowledgements

The work was supported by NSF (CMMI-1661627), ONR (N00014-17-1-2920) and MIT Institute for Soldier Nanotechnologies. We thank the assistance from Prof. Gareth McKinley and Dr Alexander Barbati for access and training in the use of the rheometer.

Notes and references

1 T. Matsunaga, T. Sakai, Y. Akagi, U.-I. Chung and M. Shibayama, SANS and SLS Studies on Tetra-Arm PEG Gels in As-Prepared and Swollen States, *Macromolecules*, 2009, **42**(16), 6245–6252.
2 T. Matsunaga, T. Sakai, Y. Akagi, U.-I. Chung and M. Shibayama, Structure Characterization of Tetra-PEG Gel by Small-Angle Neutron Scattering, *Macromolecules*, 2009, **42**(4), 1344–1351.
3 S. C. Grindy, R. Learsch, D. Mozhdehi, J. Cheng, D. G. Barrett, Z. B. Guan, P. B. Messersmith and N. Holten-Andersen, Control of hierarchical polymer mechanics with bioinspired metal-coordination dynamics, *Nat. Mater.*, 2015, **14**(12), 1210–1216.
4 K. Kawamoto, S. C. Grindy, J. Liu, N. Holten-Andersen and J. A. Johnson, Dual Role for 1,2,4,5-Tetrazines in Polymer Networks: Combining Diels-Alder Reactions and Metal Coordination To Generate Functional SupramolecularGels, *ACS Macro Lett.*, 2015, **4**(4), 458–461.
5 D. M. Loveless, S. L. Jeon and S. L. Craig, Rational Control of Viscoelastic Properties in Multicomponent Associative Polymer Networks, *Macromolecules*, 2005, **38**(24), 10171–10177.
6 W. C. Yount, D. M. Loveless and S. L. Craig, Small-molecule dynamics and mechanisms underlying the macroscopic mechanical properties of coordinatively cross-linked polymer networks, *J. Am. Chem. Soc.*, 2005, **127**(41), 14488–14496.
7 M. Rikkou-Kalourkoti, C. S. Patrickios and T. Georgiou, 6.08 – Model Networks and Functional Conetworks, in *Polymer Science: A Comprehensive Reference*, ed. K. Matyjaszewski and M. Moller, Elsevier, 2012, vol. 6, pp. 293–308.
8 G. Hild, Model networks based on 'endlinking' processes: synthesis, structure and properties, *Prog. Polym. Sci.*, 1998, **23**(6), 1019–1149.
9 Y. Akagi, T. Katashima, Y. Katsumoto, K. Fujii, T. Matsunaga, U.-I. Chung, M. Shibayama and T. Sakai, Examination of the Theories of Rubber Elasticity Using an Ideal Polymer Network, *Macromolecules*, 2011, **44**(14), 5817–5821.

10 T. Matsunaga, H. Asai, Y. Akagi, T. Sakai, U.-I. Chung and M. Shibayama, SANS Studies on Tetra-PEG Gel under Uniaxial Deformation, *Macromolecules*, 2011, **44**(5), 1203–1210.
11 M. Zhong, R. Wang, K. Kawamoto, B. D. Olsen and J. A. Johnson, Quantifying the impact of molecular defects on polymer network elasticity, *Science*, 2016, **353**(6305), 1264–1268.
12 T. Hiroi, M. Ohl, T. Sakai and M. Shibayama, Multiscale Dynamics of Inhomogeneity-Free Polymer Gels, *Macromolecules*, 2014, **47**(2), 763–770.
13 K. Hashimoto, K. Fujii, K. Nishi, T. Sakai and M. Shibayama, Nearly Ideal Polymer Network Ion Gel Prepared in pH-Buffering Ionic Liquid, *Macromolecules*, 2016, **49**(1), 344–352.
14 T. Sakai, Y. Akagi, S. Kondo and U. Chung, Experimental verification of fracture mechanism for polymer gels with controlled network structure, *Soft Matter*, 2014, **10**(35), 6658–6665.
15 M. J. Webber, E. A. Appel, E. W. Meijer and R. Langer, Supramolecular biomaterials, *Nat. Mater.*, 2016, **15**(1), 13–26.
16 C. J. Kloxin and C. N. Bowman, Covalent adaptable networks: smart, reconfigurable and responsive network systems, *Chem. Soc. Rev.*, 2013, **42**(17), 7161–7173.
17 H. Wang and S. C. Heilshorn, Adaptable hydrogel networks with reversible linkages for tissue engineering, *Adv. Mater.*, 2015, **27**(25), 3717–3736.
18 L. Voorhaar and R. Hoogenboom, Supramolecular polymer networks: hydrogels and bulk materials, *Chem. Soc. Rev.*, 2016, **45**(14), 4013–4031.
19 E. B. Stukalin, L. H. Cai, N. A. Kumar, L. Leibler and M. Rubinstein, Self-Healing of Unentangled Polymer Networks with Reversible Bonds, *Macromolecules*, 2013, **46**(18), 7525–7541.
20 F. Herbst, D. Dohler, P. Michael and W. H. Binder, Self-healing polymers *via* supramolecular forces, *Macromol. Rapid Commun.*, 2013, **34**(3), 203–220.
21 O. Chaudhuri, L. Gu, D. Klumpers, M. Darnell, S. A. Bencherif, J. C. Weaver, N. Huebsch, H. P. Lee, E. Lippens, G. N. Duda and D. J. Mooney, Hydrogels with tunable stress relaxation regulate stem cell fate and activity, *Nat. Mater.*, 2016, **15**(3), 326–334.
22 X. Zhao, N. Huebsch, D. J. Mooney and Z. Suo, Stress-relaxation behavior in gels with ionic and covalent cross-links, *J. Appl. Phys.*, 2010, **107**(6), 63509.
23 N. Holten-Andersen, M. J. Harrington, H. Birkedal, B. P. Lee, P. B. Messersmith, K. Y. C. Lee and J. H. Waite, pH-induced metal-ligand cross-links inspired by mussel yield self-healing polymer networks with near-covalent elastic moduli, *Proc. Natl. Acad. Sci. U. S. A.*, 2011, **108**(7), 2651–2655.
24 X. Zhao, Multi-scale multi-mechanism design of tough hydrogels: building dissipation into stretchy networks, *Soft Matter*, 2014, **10**(5), 672–687.
25 S. S. Nabavi, P. Fratzl and M. A. Hartmann, Energy dissipation and recovery in a simple model with reversible cross-links, *Phys. Rev. E: Stat., Nonlinear, Soft Matter Phys.*, 2015, **91**(3), 032603.
26 J. Blass, M. Albrecht, G. Wenz, Y. N. Zang and R. Bennewitz, Single-molecule force spectroscopy of fast reversible bonds, *Phys. Chem. Chem. Phys.*, 2017, **19**(7), 5239–5245.
27 H. Gao, W. Shi and L. B. Freund, Mechanics of receptor-mediated endocytosis, *Proc. Natl. Acad. Sci. U. S. A.*, 2005, **102**(27), 9469–9474.
28 G. Bell, Models for the specific adhesion of cells to cells, *Science*, 1978, **200**(4342), 618–627.
29 F. Tanaka and S. F. Edwards, Viscoelastic properties of physically crosslinked networks. Transient network theory, *Macromolecules*, 1992, **25**(5), 1516–1523.
30 F. Tanaka and S. F. Edwards, Viscoelastic properties of physically crosslinked networks. Part 2: Dynamic Mechanical Moduli, *J. Non-Newtonian Fluid Mech.*, 1992, **43**(2–3), 273–288.
31 K. E. Feldman, M. J. Kade, E. W. Meijer, C. J. Hawker and E. J. Kramer, Model Transient Networks from Strongly Hydrogen-Bonded Polymers, *Macromolecules*, 2009, **42**(22), 9072–9081.
32 D. Xu and S. L. Craig, Scaling Laws in Supramolecular Polymer Networks, *Macromolecules*, 2011, **44**(13), 5465–5472.
33 V. Yesilyurt, M. J. Webber, E. A. Appel, C. Godwin, R. Langer and D. G. Anderson, Injectable Self-Healing Glucose-Responsive Hydrogels with pH-Regulated Mechanical Properties, *Adv. Mater.*, 2016, **28**(1), 86–91.
34 V. Yesilyurt, A. M. Ayoob, E. A. Appel, J. T. Borenstein, R. Langer and D. G. Anderson, Mixed Reversible Covalent Crosslink Kinetics Enable Precise, Hierarchical Mechanical Tuning of Hydrogel Networks, *Adv. Mater.*, 2017, 1605947.
35 D. E. Apostolides, T. Sakai and C. S. Patrickios, Dynamic Covalent Star Poly(ethylene glycol) Model Hydrogels: A New Platform for Mechanically Robust, Multifunctional Materials, *Macromolecules*, 2017, **50**(5), 2155–2164.
36 N. Holten-Andersen, B. P. Lee, P. B. Messersmith, J. H. Waite and K. Y. C. Lee, Mussel-Inspired Self-Healing Hydrogels, *Biophys. J.*, 2010, **98**(3), 604a.
37 D. G. Barrett, D. E. Fullenkamp, L. H. He, N. Holten-Andersen, K. Y. C. Lee and P. B. Messersmith, pH-Based Regulation of Hydrogel Mechanical Properties Through Mussel-Inspired Chemistry and Processing, *Adv. Funct. Mater.*, 2013, **23**(9), 1111–1119.
38 W. C. Yount, D. M. Loveless and S. L. Craig, Strong Means Slow: Dynamic Contributions to the Bulk Mechanical Properties of Supramolecular Networks, *Angew. Chem.*, 2005, **117**(18), 2806–2808.
39 M. Rubinstein and A. N. Semenov, Dynamics of Entangled Solutions of Associating Polymers, *Macromolecules*, 2001, **34**(4), 1058–1068.
40 D. Amin, A. E. Likhtman and Z. Wang, Dynamics in Supramolecular Polymer Networks Formed by Associating Telechelic Chains, *Macromolecules*, 2016, **49**(19), 7510–7524.
41 B. J. Gold, C. H. Hövelmann, N. Lühmann, N. K. Székely, W. Pyckhout-Hintzen, A. Wischnewski and D. Richter, Importance of Compact Random Walks for the Rheology of Transient Networks, *ACS Macro Lett.*, 2017, **6**(2), 73–77.
42 R. Merkel, P. Nassoy, A. Leung, K. Ritchie and E. Evans, Energy landscapes of receptor-ligand bonds explored with dynamic force spectroscopy, *Nature*, 1999, **397**(6714), 50–53.
43 E. Evans, Probing the relation between force – lifetime – and chemistry in single molecular bonds, *Annu. Rev. Biophys. Biomol. Struct.*, 2001, **30**, 105–128.

44 G. Springsteen and B. Wang, A detailed examination of boronic acid–diol complexation, *Tetrahedron*, 2002, **58**(26), 5291–5300.
45 J. Yan, G. Springsteen, S. Deeter and B. Wang, The relationship among pKa, pH, and binding constants in the interactions between boronic acids and diols—it is not as simple as it appears, *Tetrahedron*, 2004, **60**(49), 11205–11209.
46 Y. Furikado, T. Nagahata, T. Okamoto, T. Sugaya, S. Iwatsuki, M. Inamo, H. D. Takagi, A. Odani and K. Ishihara, Universal reaction mechanism of boronic acids with diols in aqueous solution: kinetics and the basic concept of a conditional formation constant, *Chemistry*, 2014, **20**(41), 13194–13202.
47 J. W. Tomsho and S. J. Benkovic, Elucidation of the mechanism of the reaction between phenylboronic acid and a model diol, Alizarin Red S, *J. Org. Chem.*, 2012, **77**(5), 2098–2106.
48 J. Y. Sun, X. H. Zhao, W. R. K. Illeperuma, O. Chaudhuri, K. H. Oh, D. J. Mooney, J. J. Vlassak and Z. G. Suo, Highly stretchable and tough hydrogels, *Nature*, 2012, **489**(7414), 133–136.
49 H. Yuk, T. Zhang, G. A. Parada, X. Liu and X. Zhao, Skin-inspired hydrogel-elastomer hybrids with robust interfaces and functional microstructures, *Nat. Commun.*, 2016, **7**, 12028.
50 H. Yuk, T. Zhang, S. Lin, G. A. Parada and X. Zhao, Tough bonding of hydrogels to diverse non-porous surfaces, *Nat. Mater.*, 2016, **15**(2), 190–196.
51 T. Zhang, H. Yuk, S. Lin, G. Parada and X. Zhao, Tough and Tunable Adhesion of Hydrogels: Experiments and Models, *Acta Mech. Sin.*, 2017, 543–554.
52 S. Lin, H. Yuk, T. Zhang, G. A. Parada, H. Koo, C. Yu and X. Zhao, Stretchable Hydrogel Electronics and Devices, *Adv. Mater.*, 2016, **28**(22), 4497–4505.
53 X. Liu, H. Yuk, S. Lin, G. A. Parada, T. C. Tang, E. Tham, C. de la Fuente-Nunez, T. K. Lu and X. Zhao, 3D Printing of Living Responsive Materials and Devices, *Adv. Mater.*, 2018, **30**(4), 1704821.
54 G. A. Parada, H. Yuk, X. Liu, A. J. Hsieh and X. Zhao, Impermeable Robust Hydrogels *via* Hybrid Lamination, *Adv. Healthcare Mater.*, 2017, **6**(19), 1700520.
55 H. Yuk, S. Lin, C. Ma, M. Takaffoli, N. X. Fang and X. Zhao, Hydraulic hydrogel actuators and robots optically and sonically camouflaged in water, *Nat. Commun.*, 2017, **8**, 14230.
56 Q. C. Li, D. G. Barret, P. B. Messersmith and N. Holten-Andersen, Controlling Hydrogel Mechanics *via* Bio-Inspired Polymer-Nanoparticle Bond Dynamics, *ACS Nano*, 2016, **10**(1), 1317–1324.
57 D. Mozhdehi, J. A. Neal, S. C. Grindy, Y. Cordeau, S. Ayala, N. Holten-Andersen and Z. B. Guan, Tuning Dynamic Mechanical Response in Metallopolymer Networks through Simultaneous Control of Structural and Temporal Properties of the Networks, *Macromolecules*, 2016, **49**(17), 6310–6321.
58 R. Wang, M. K. Sing, R. K. Avery, B. S. Souza, M. Kim and B. D. Olsen, Classical Challenges in the Physical Chemistry of Polymer Networks and the Design of New Materials, *Acc. Chem. Res.*, 2016, **49**(12), 2786–2795.
59 S. Tang and B. D. Olsen, Relaxation Processes in Supramolecular Metallogels Based on Histidine–Nickel Coordination Bonds, *Macromolecules*, 2016, **49**(23), 9163–9175.
60 R. Wang, T.-S. Lin, J. A. Johnson and B. D. Olsen, Kinetic Monte Carlo Simulation for Quantification of the Gel Point of Polymer Networks, *ACS Macro Lett.*, 2017, **6**(12), 1414–1419.
61 T.-S. Lin, R. Wang, J. A. Johnson and B. D. Olsen, Topological Structure of Networks Formed from Symmetric Four-Arm Precursors, *Macromolecules*, 2018, **51**(3), 1224–1231.
62 Y. Liang, L. Li, R. A. Scott and K. L. Kiick, Polymeric Biomaterials: Diverse Functions Enabled by Advances in Macromolecular Chemistry, *Macromolecules*, 2017, **50**(2), 483–502.
63 O. Chaudhuri, Viscoelastic hydrogels for 3D cell culture, *Biomater. Sci.*, 2017, **5**(8), 1480–1490.
64 G. R. Gossweiler, G. B. Hewage, G. Soriano, Q. Wang, G. W. Welshofer, X. Zhao and S. L. Craig, Mechanochemical Activation of Covalent Bonds in Polymers with Full and Repeatable Macroscopic Shape Recovery, *ACS Macro Lett.*, 2014, **3**(3), 216–219.
65 Q. Wang, G. R. Gossweiler, S. L. Craig and X. Zhao, Mechanics of mechanochemically responsive elastomers, *J. Mech. Phys. Solids*, 2015, **82**, 320–344.
66 C. W. Macosko and D. R. Miller, A New Derivation of Average Molecular Weights of Nonlinear Polymers, *Macromolecules*, 1976, **9**(2), 199–206.
67 N. R. Langley and K. E. Polmanteer, Relation of elastic modulus to crosslink and entanglement concentrations in rubber networks, *J. Polym. Sci., Polym. Phys. Ed.*, 1974, **12**(6), 1023–1034.
68 M. S. Green and A. V. Tobolsky, A New Approach to the Theory of Relaxing Polymeric Media, *J. Chem. Phys.*, 1946, **14**(2), 80–92.
69 M. Rubinstein and R. Colby, *Polymer Physics*, Oxford University Press, 2003.
70 Y. Guan and Y. Zhang, Boronic acid-containing hydrogels: synthesis and their applications, *Chem. Soc. Rev.*, 2013, **42**(20), 8106–8121.
71 P. C. Hiemenz and T. P. Lodge, *Polymer Chemistry*, Taylor and Francis Group, Boca Raton, FL, 2nd edn, 2007.
72 M. Miyara, I. Takashima, K. Sasaki, R. Kita, N. Shinyashiki and S. Yagihara, Dynamics of uncrystallized water in partially crystallized poly(ethylene glycol)–water mixtures studied by dielectric spectroscopy, *Polym. J.*, 2017, **49**(6), 511–518.
73 H. Monajemi, M. H. Cheah, V. S. Lee, S. M. Zain and W. A. T. W. Abdullah, On the kinetics and reaction mechanisms of boronic acid in interaction with diols for non-enzymatic glucose monitoring applications: a hybrid DFT study, *RSC Adv.*, 2014, **4**(21), 10505.
74 S. W. Sinton, Complexation chemistry of sodium borate with poly(vinyl alcohol) and small diols: a boron-11 NMR study, *Macromolecules*, 1987, **20**(10), 2430–2441.

